Combined Kinetic, and Theoretical Approaches for the Study of the SEAr Reactions of 2-(2',4',6'-trinitrophenyl)-4,6-dinitrobenzotriazole 1-oxide with 5-R-substituted Indoles in Acetonitrile

Ons Amamou

　Université de Monastir Faculté des Sciences de Monastir: Universite de Monastir Faculte des Sciences de Monastir

Amel Hedhli

　Université de Monastir Faculté des Sciences de Monastir: Universite de Monastir Faculte des Sciences de Monastir

Takwa Slama

　University of Monastir Faculty of Sciences of Monastir: Universite de Monastir Faculte des Sciences de Monastir

Sahbi Ayachi

　Université de Monastir Faculté des Sciences de Monastir: Universite de Monastir Faculte des Sciences de Monastir

Taoufik Boubaker

　boubaker_taoufik@yahoo.fr

　University of Monastir: Universite de Monastir

Combined Kinetic, and Theoretical Approaches for the Study of the SEAr Reactions of 2-(2',4',6'-trinitrophenyl)-4,6-dinitrobenzotriazole 1-oxide with 5-R-substituted Indoles in Acetonitrile

Ons Amamou,[a] Amel Hedhli,[a] Takwa Slama,[a] Sahbi Ayachi,[b] and Taoufik Boubaker[a,*]

[a]Laboratoire de Chimie Hétérocyclique, Produits Naturels et Réactivité (LR11SE39), Faculté des Sciences de Monastir, Université de Monastir, Avenue de l'Environnement, 5019 Monastir, Tunisie.
[b]Laboratoire de Physico-chimie des Matériaux (LR01ES19), Faculté des Sciences, Université de Monastir, Avenue de l'Environnement, 5019 Monastir, Tunisie.

Corresponding author: Prof. Taoufik Boubaker
e-mail: boubaker_taoufik@yahoo.fr

Phone : 00 216 98 65 21 21

ABSTRACT

We present a kinetic and theoretical study of nucleophilic addition reactions involving 2-(2',4',6'-trinitrophenyl)-4,6-dinitrobenzotriazole 1-oxide **1** with a series of 5-R-substituted indoles **2a-e** (R = CN, Cl, H, Me and NH_2) in acetonitrile at 20 °C. Single electron transfer (SET) mechanism was proposed and confirmed by the agreement between the rate constants (k) and the oxidation potentials (E_p^{ox}) of these series of indoles. Using Mayr's equation, the electrophilicity parameter (*E)* of **1** at C-7 position is derived and compared with the same parameter estimate using empirical equation *E vs*. pK_a. Density Functional Theory (DFT) calculations were performed to confirm the suggested reaction mechanisms and elucidate the origin of the electrophilic reactivity of **1**. Notably, a linear correlation ($R^2 = 0.9957$) between the experimental nucleophilicity (*N*) and the theoretical model of nucleophilicity (ω^{-1}) determined in this work of various 5-R-substituted indoles has been obtained and discussed.

1. Introduction

In our previous research, we conducted a kinetic study on the reactions involving a series of electron-deficient aromatic and heteroaromatic substrates, such as 1,3,5-trinitrobenzene, nitrobenzofuroxans and nitrobenzofurazans, with a diverse range of nucleophiles (including pyrrole, indoles and enamines) (Lakhdar et al. 2006). Our findings revealed that the derived second-order rate constants (k, M^{-1} s^{-1}) are effectively described by the linear-free energy relationship formulated by Mayr (Eq 1) (Mayr et al. 1994; Li et al. 2022; Hensinger et al. 2023). In this equation, s_N and N represent nucleophile-specific parameters, and E is an electrophilicity parameter.

$$\log k \ (20 \ °C) = s_N \ (E + N) \tag{1}$$

It was further demonstrated that the resulting electrophilic reactivities conform to the correlation depicted by Eq. (2), (Lakhdar et al. 2006; Terrier et al. 2005) wherein $pK_a^{H_2O}$ refers to the covalent hydration of this series of electrophiles.

$$E = -3.20 - 0.662 \ pK_a^{H_2O} \tag{2}$$

To expand the applicability of eq (1), this paper present a study of the σ-complexation reactions of 2-(2',4',6'-trinitrophenyl)-4,6-dinitrobenzotriazole 1-oxide **1** with a series of 5-R-substituted indoles **2a-e** in acetonitrile at 20 °C (Scheme 1). As observed, the validity of eq (2) is confirmed by comparing the electrophilicity parameter E of benzotriazole 1 obtained in this work with that estimated previously according eq (2). The basicity effect of indoles **2a-e** and electronic effect of the substituent R on reactivity and mechanism have been examined and discussed based on linear free-energy relationships. Additionally, computational investigations at the density functional theory (DFT) level have been undertaken to discuss the proposed mechanism. On the other hand, the theoretical nucleophilicity (ω^{-1}) pattern of a series of 5-R-substituted indoles, described in terms of Parr's approach (Parr et al. 1999), is compared with the experimental nucleophilicity (N) measured using equation of Mayr (Lakhdar et al. 2006).
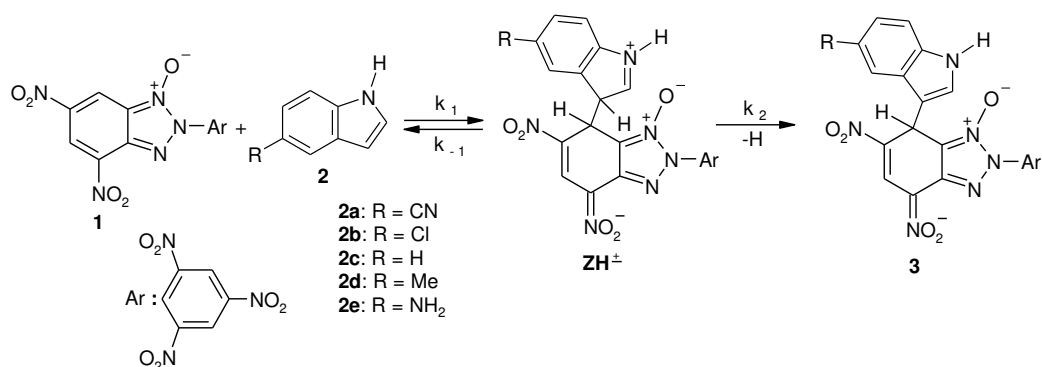
Scheme 1. σ-complexation reactions of the 2-(2',4',6'-trinitrophenyl)-4,6-dinitrobenzotriazole 1-oxide **1** with indoles **2a-e** in acetonitrile at 20 °C.

2. Results and Discussion

2.1. Structural studies of the σ-complexes **3a-e**

The UV-visible absorption spectrum of benzotriazole **1** exhibits a maximum at 404 nm in acetonitrile. Upon addition a dilute solution of indole **2a** to a yellow solution of benzotriazole **1** in acetonitrile, an orange solution is produced, displaying a new absorption band, peaking at 478 nm and feauturing an isosbestic point at 435 nm (Figure 1). It is notewoirthy that benzotriazole **1** does not form a σ-adduct of C-1' attack with any of the investigated indoles under the reaction conditions; only attack at C-7 is observed, resulting in the formation of the σ-adduct **3.**
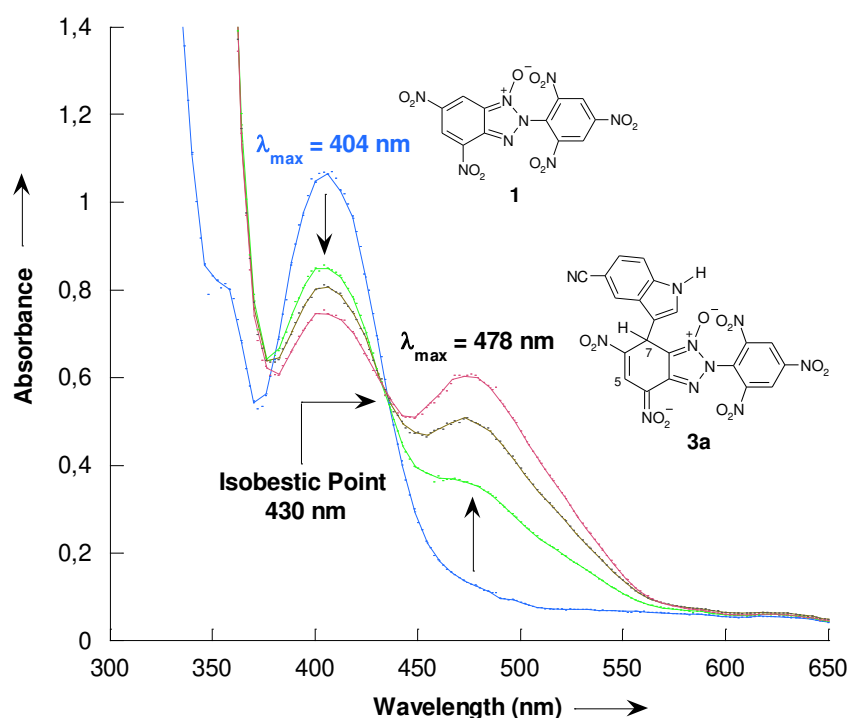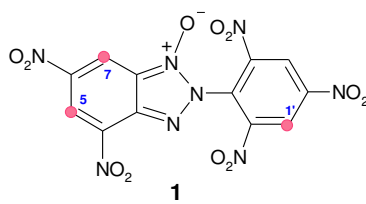

Figure 1. Time dependence of the electronic absorption spectrum of benzotriazole 1-oxide **1** (2 x 10^{-4} mol L^{-1}) in the presence of 5-cyanoindole **2a** (4 x 10^{-2} mol L^{-1}) in acetonitrile at 20 °C.

4

To validate the experimental electrophilic reactivity at the C-7 position of the benzotriazole **1**, we conducted calculations on the local electron spin densities (LESDs) (Ayachi et al. 2006) at various atomic sites of this electrophile **1**. It is crucial to note that the determined relative values are highly significant, particularly in predicting nucleophilic attack sites. In this context, we have identified potential nucleophilic attack sites along with their DESDs. Our LSEDs results compiled in Table 1 reveal that within the considered benzotriazole, the **C-7** position exhibits a greater degree of electron localization (higher LSEDs value) compared to the electron localization at **C-1'**. This observation suggests a preference for nucleophilic attack at the **C-7** center over the **C-1'** center.

Table 1. Calculated Milliken charges and local electron spin densities (LESDs) at various atomic sites of the electrophile **1** in acetonitrile.

	Carbon	Milliken Charges	LESDs
	5	0.067	−0.011
	7	0.158	0.030
	1'	0.106	0.003

Additionnally, we optimized the geometries of the thre proposed isomers, namely **3c**, **4c**, and **5c** (refer to Figure 2), to examine their optical UV-vis absorption spectra using the same calculation method as described earlier. The UV-vis optical absorption spectra of the anionic σ-complexes **3c**, **4c** and **5c** are depected schematically in Figure 3. Notably, the simulated UV-vis optical absorption spectrum of σ-adduct **3a** aligns with the experimental UV-vis absorption spectrum obtained from the investigation of the nucleophilic addition reaction of 4,6-dinitrobenzotriazole 1-oxide **1** with indole, as discussed previously.

In conclusion, B3LYP/6-311g(d,p) calculations indicate a preference for indole addition to benzotriazole through nucleophilic attack on the **C-7** position rather than **C-1'** position.
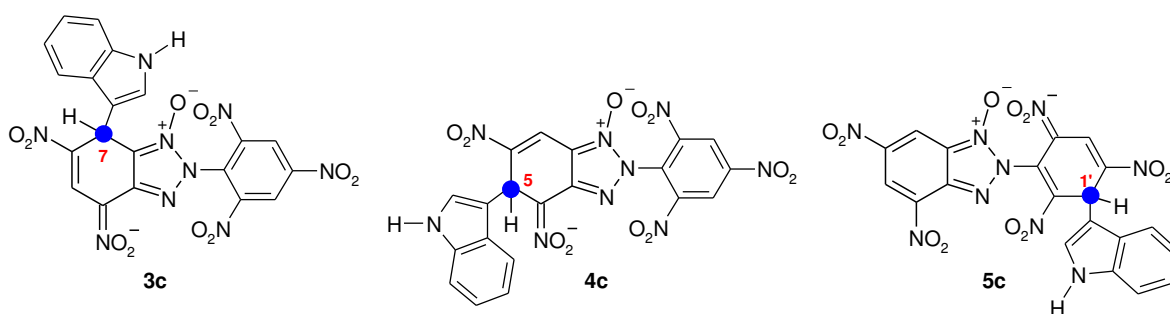
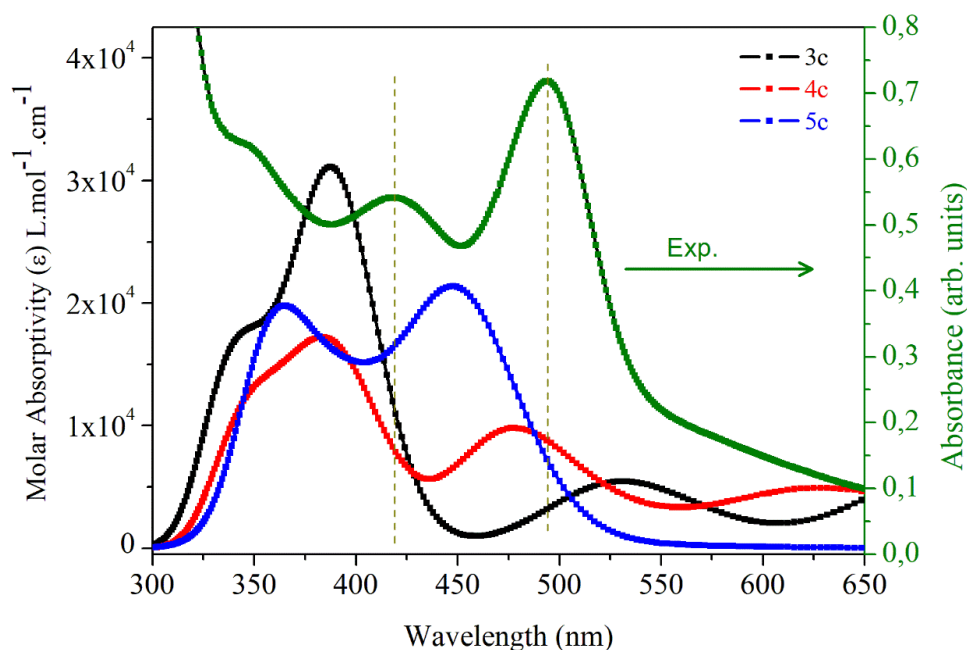**Figure 2.** Structures of the anionic σ-complexes **3c**, **4c** and **5c** studied and the labeling of positions.

Figure 3. Absorption spectra of benzotriazole **1** (3×10^{-5} M^{-1} s^{-1}) and its adducts **3c**, **4c** and **5c** in acetonitrile solution at 20 °C.

2.2. Kinetic Investigations: Reactions of Benzotriazole 1-oxide **1** *with Indoles* **2a-e**

The reactions of the of 2-(2',4',6'-trinitrophenyl)-4,6-dinitrobenzotriazole 1-oxide **1** with a series of 5-R-substituted indoles **2a-e** were conducted in acetonitrile solution at 20 °C and monitored by UV-vis spectroscopy at or close to the absorption maximum of one of the resulting σ-adducts **3a-e** (478 nm < λ_{max} < 495 nm). Experiments were carried out by directly mixing a 3×10^{-5} mol L^{-1} solution of benzotriazole **1** with a large excess of indoles **2a-e** (2×10^{-3} to 3×10^{-1} mol L^{-1}). In all cases, the apparent first-order rate constants (k_{obsd}) were determined through the kinetic analyses described by Equation (3) (Terrier et al. 1993).

$$k_{obsd} = \frac{k_1 \, k_2}{k_{-1} + k_2}[\text{Indole}] \qquad (3)$$

6

When the relation $k_{-1} \ll k_2$ is satisfied, Eq (3) is rewritten as Eq (4), suggesting that the k_{obsd} is first order with respect to nucleophile concentration where k_1 is the second-order rate constant for the indole addition to the benzotriazole **1**. In this regard, we note that Terrier and co-workers (Terrier et al. 1993) have studied the reactions of 4,6-dinitrobenzofuroxan with a series of 5-R-substituted indoles in various solvents. Their findings revealed that the initial nucleophile attack is also a rate-determining step.

$$k_{obsd} = k_1 \text{ [Indole]} \qquad (4)$$

Plots of k_{obsd} versus the concentrations of the indoles **2a-e** resulted straight lines with slopes representing k_1, as illustrated in Figure 4 for one example. These findings align with the expectations from Eq (4). The second-order rate constants k_1 are compiled in Table 2.
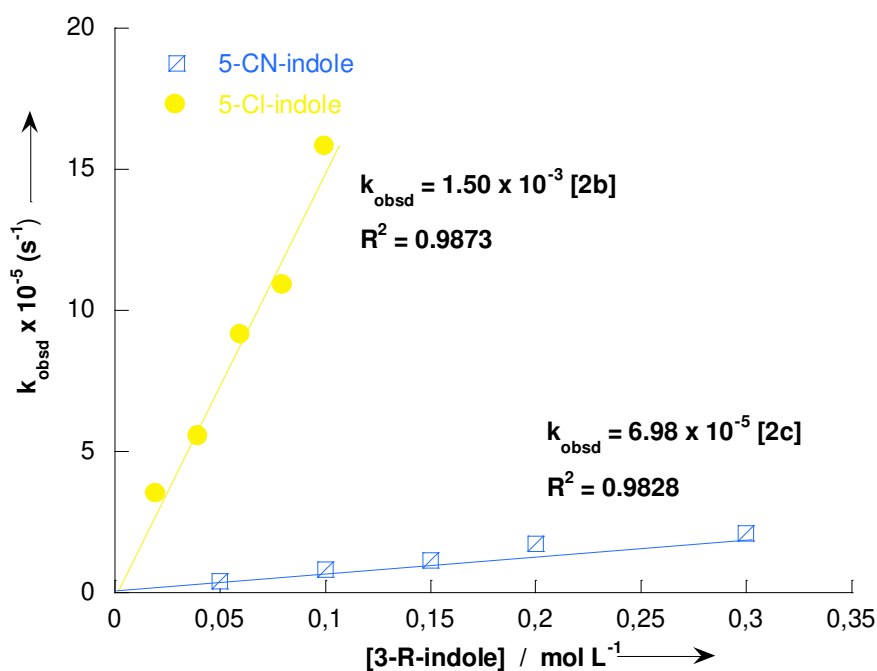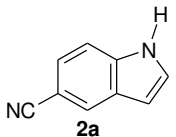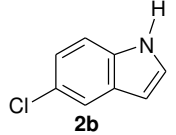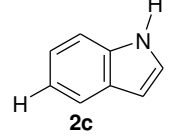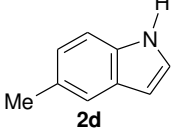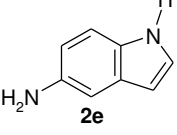

Figure 4. Plots of the first-order rate constants k_{obsd} *vs*. the concentration of indoles **2a** and **2b** in acetonitrile solution at 20 °C.

Table 2. Summary of second-order rate constants for addition reactions of 5-R-substituted indoles **2a-e** with benzotriazole **1** in acetonitrile solution at 20 °C.

Nucleophile	k_1 (M^{-1} s^{-1}) [a]	pK_{aH} [c]	E_p^{ox} [d] (V *vs* NHE)	N / s_N [e]
2a	6.98×10^{-5}	−6.00	1.64	2.83 / 1.10
2b	1.50×10^{-3}	−4.53	1.30	4.42 / 1.10
2c	8.91×10^{-2} 1.97×10^{-2} [b]	−3.46	1.10	5.55 / 1.09 [f]
2d	2.60×10^{-1}	−3.30	0.94	6.00 / 1.10
2e	2.43	−1.76	0.56	7.22 / 1.10

[a]Values of k_1 are determined in this work from the slope of plots of k_{obsd} *vs*. [5-R-indole] in CH$_3$CN.
[b]Value of indole **2c** is determined in this work from the slope of plots of k_{obsd} *vs*. [indole] in CH$_2$Cl$_2$.
[c]pK$_a$ values for conjugated acid of 5-R-substituted indoles **2a-e** in water taken from ref (Lakhdar et al. 2006).
[d]E_p^{ox} values for indole **2a-e** in CH$_3$CN solution were taken from ref (Jennings et al. 1997).
[e]N and s_N values in CH$_3$CN were taken from ref (Lakhdar et al. 2006).
[f]N and s_N values of indole **2c** in CH$_2$Cl$_2$ were taken from ref (Lakhdar et al. 2006).

2.3. Effect of indole basicity and mechanism

The direct relationship between the σ-complexation reaction of 4,6-dinitrobenzotriazole 1-oxide **1** with 5-R-substituted indoles **2a-e** is illustrated in Figure 5. In this Figure, the second-order rate constant is plotted against the pK_{aH} values of the conjugate acids of the indoles **2a-e** in water (Lakhdar et al. 2006), as listed in Table 2. The linear correlation is mathematically represented by Equation (5), yielding a correlation coefficient of 0.9814.

$$\log k_1 = 2.68 + 1.13\ pK_{aH} \tag{5}$$

It is interesting to note that the β_{nuc} value for the reactions of benzotriazole **1** (i.e., β_{nuc} = 1.13) is notably higher than those reported for the σ-complexation reactions (Boubaker et al 2002 ; Gabsi et al. 2018; Buncel et al. 2010; Boubaker et al. 2023; El Guesmi et al. 2009; El Guesmi et al. 2010). As discussed by various authors, (Mahdhaoui et al. 2016; Jamaoui et al. 2013;

8

Terrier et al. 2003; Raissi et al. 2017; Raissi et al. 2021; Hunter et al. 1995; El Guesmi et al. 2013; Ben Salah et al. 2017) a large β_{nuc} value align with a single electron transfer (SET) process. The analogous mechanism was previously postulated in the σ-complexation of 4-nitrobenzofurazan **6** with 4-X-substituted phenoxide anions (X = OCH$_3$, CH$_3$, H and Cl) in aqueous solution by Ben Salah and co-works (Ben Salah et al. 2017). More recently, Slama and collaborators demostrated that nucleophilic aromatic substitution reactions (S$_N$Ar) of 2-methoxy-3,5-dinitropyridine **7** with secondary cyclic amines in acetonitrile solution proceed through a mechanism involving an electron transfer of electrons (Slama et al. 2024) .
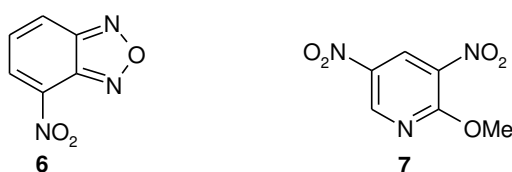
It appears that our σ-complexation reactions of 4,6-benzotriazole **1** with indoles **2** in CH$_3$CN proceed via SET mechanism, as depicted in Scheme 2. In this mechanism, the formation of the σ-adducts **3a-e** involves an initial (fast) electron-transfer from the indoles **2a-e** to the electrophile **1,** followed by a subsequent (slow) coupling of the resulting cation and anion radicals within the solvent cage. This process leads, to the formation of the zwitterionic σ-complex **ZH$^\pm$** (Terrier et al. 2013).
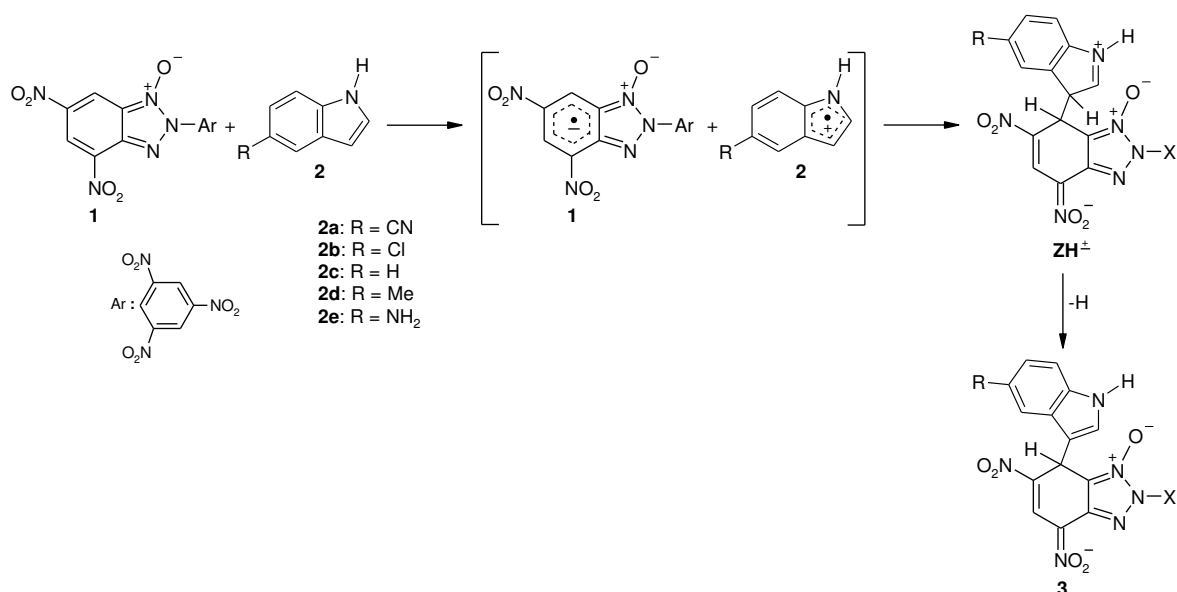
Scheme 2. Proposed mechanistic pathway for the reactions of benzotriazole 1-oxide **1** with indoles **2a-e** in acetonitrile at 20 °C.
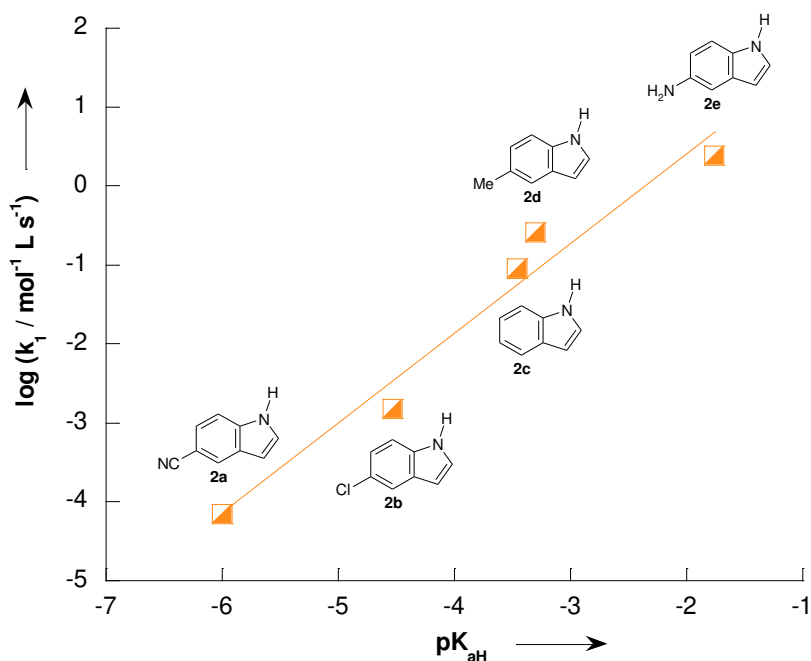
Figure 5. Correlation of log k_1 for the reactions of the 2-(2',4',6'-trinitrophenyl)-4,6-dinitrobenzotriazole 1-oxide **1** with 5-R-substituted indoles **2** versus the pK_{aH} values of their conjugated acids.

To gain a better understanding of the formation process of the final σ-adduct, benzotriazole-indole, we initially explored the feasibility of the synthetic reaction between the fundamental starting materials: benzotriazole **1** and indoles **2a-e** using theoretical calculations through Density Functional Theory (DFT). This preliminary study aimed to optimize the geometrically stable structures in their ground states (S_0), theoretically determine their associated molecular orbital energy levels (HOMO and LUMO), and identify which could function as the electrophile or nucleophile, essentially forming donor-acceptor pairs often referred to as a push-pull electron transfer system. In this context, we determined the density of states (DOS) spectra for the two geometries, as depicted in Figure 6 (a) and (b).

The distribution of electronic states density (DOS) is evident, highlighting difference between both sub-units. In Figure 6c, we have graphically depicted their electronic structures, illustrating all HOMO and LUMO band energy levels within the 0-10 eV energy range (with 0 eV representing the vacuum level). The energy diagram (see Figure 6c), characterized by the tilting of the HOMO and LUMO levels, reveals that the indole exhibits relatively high-lying highest occupied molecular orbital (HOMO) and lowest unoccupied molecular orbital (LUMO) energy levels compared to benzotriazole **1**.

In other words, the combined structure implies the presence of a molecular system with an electron donor-acceptor (D/A) architecture. This configuration facilitates electron transfer during the coupling process. Previous studies have established that the electron donor acts as a nucleophile, while the electron acceptor group functions as an electrophile (Safi et al. 2023; Zhuo et al. 2012; Miar et al. 2021). Examining of the molecular orbitals (HOMO and LUMO) graphs reveals that the electrophilic moiety on the right, the trinitophenyl group, lacks electrons, indicating its high electron-accepting nature in the event of a nucleophilic reaction.
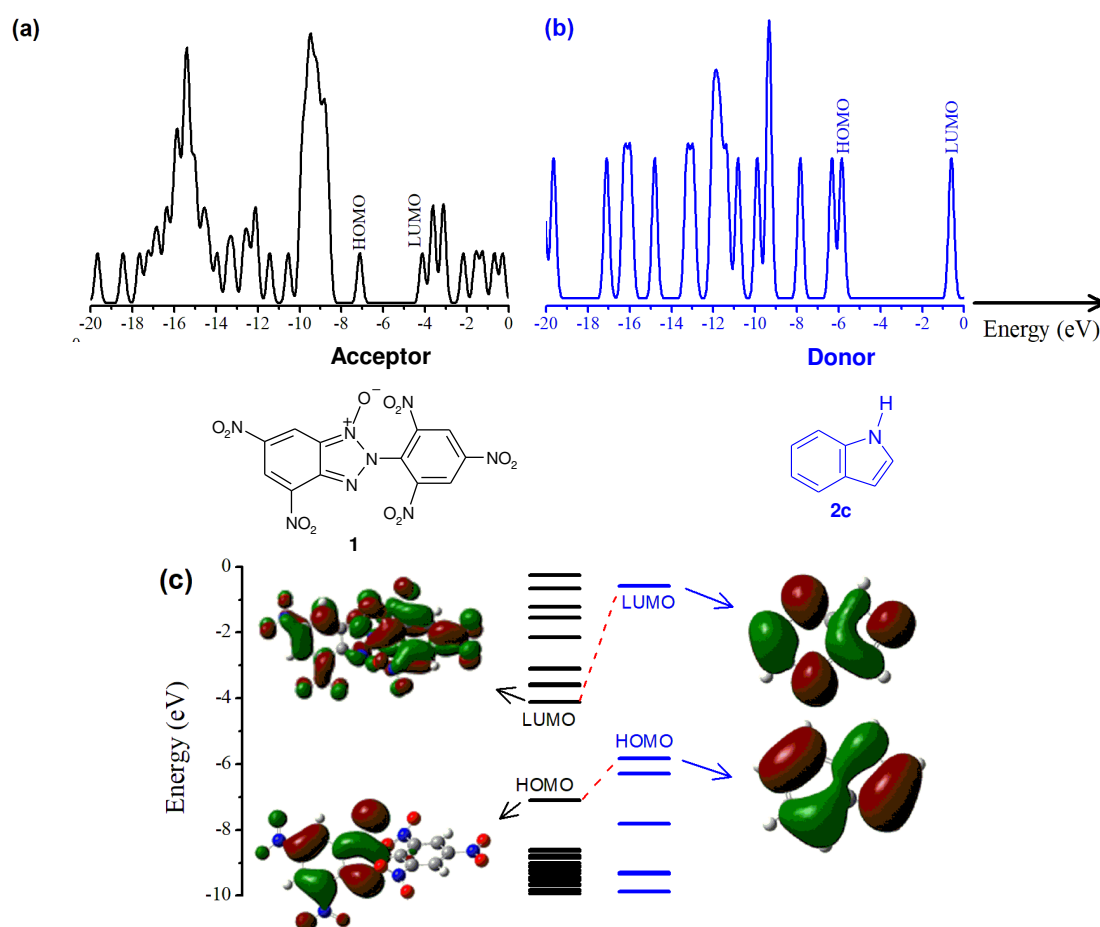
Figure 6. Density of States (DOS) diagrams, depected in (a) and (b) for the **1** and **2c** compounds, respectively. Their corresponding energy band diagrams and contour plots of HOMO and LUMO are also given (c).

This mechanistic proposal receives addional support from the observation that the plot of (log k_1) vs the oxidation peak potentials E_p^{OX} values of the indoles radical cations measured in acetonitrile (Jennings et al. 1997) is linear (Figure 7), with a correlation coefficient of 0.9733.
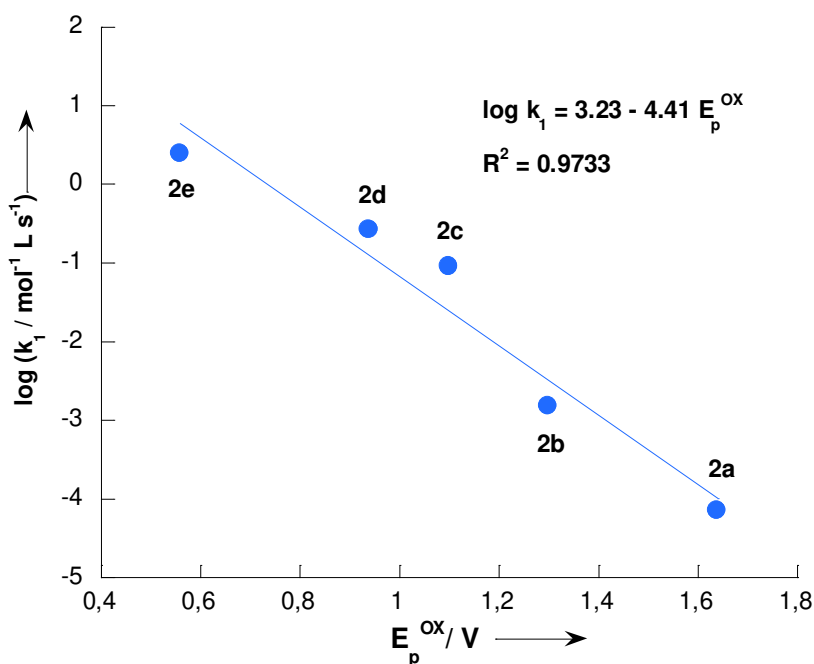
Figure 7. The influence of the oxidation peak potentials E_p^{OX} of 5-R-substituted indoles **2a-e** on the rate constants of reactions of 2-(2',4',6'-trinitrophenyl)-4,6-dinitrobenzotriazole 1-oxide **1** with these series of indoles **2** in CH_3CN at 20 °C. The identity of points is given in Table 2.

2.4. Quantification of electrophilicity E of benzotriazole 1-oxide 1

As shown in Table 2, the reactivity of the 4,6-dinitrobenzotriazole 1-oxide **1** with the reference nucleophiles **2a-e** decreases as their nucleophilicity decreases. For example, k_1 decreases from 2.43 to 6.98 x 10^{-5} mol^{-1} L s^{-1} as the nucleophilicity parameter N of indole (Lakhdar et al. 2006) decreases from 7.22 to 2.83, respectively. This nucleophilicity-dependent effect on reactivity is illustrated in Figure 8. A highly linear relationship is observed when plotting $(\log k_1)/s_N$ values against the nucleophilicity parameters N determined in acetonitrile of 5-R-substituted indoles **2a-e**. This behavior confirms the applicability of Mayr's approach to these σ-complexation reactions (Corral-Bautista et al. 2015; Necibi et al. 2020; Justel et al. 2021; Ben Salah et al. 2020; Timofeeva et al. 2018; Rammah et al. 2021; Echaieb et al. 2014; Gabsi et al. 2016 Raissi et al. 2022). From the intercept of this line with the ordinate axis, the reactivity of electrophile **1** is derived ($E = -6.87$), which compares well to the previously reported value of -7.63 (Terrier et al. 2005). The latter was calculated using the correlation $E = -3.20 - 0.662$ $pK_a^{H_2O}$ (Terrier et al. 2005), with a $pK_a^{H_2O}$ value of 6.70 associated with the covalent hydration of electrophile (Boubaker et al. 2002). More recently,

a value of $E = -5.97$ has also been estimated by Rammah and co-workers (Rammah et al. 2022) using both approach of Mayr and Parr.
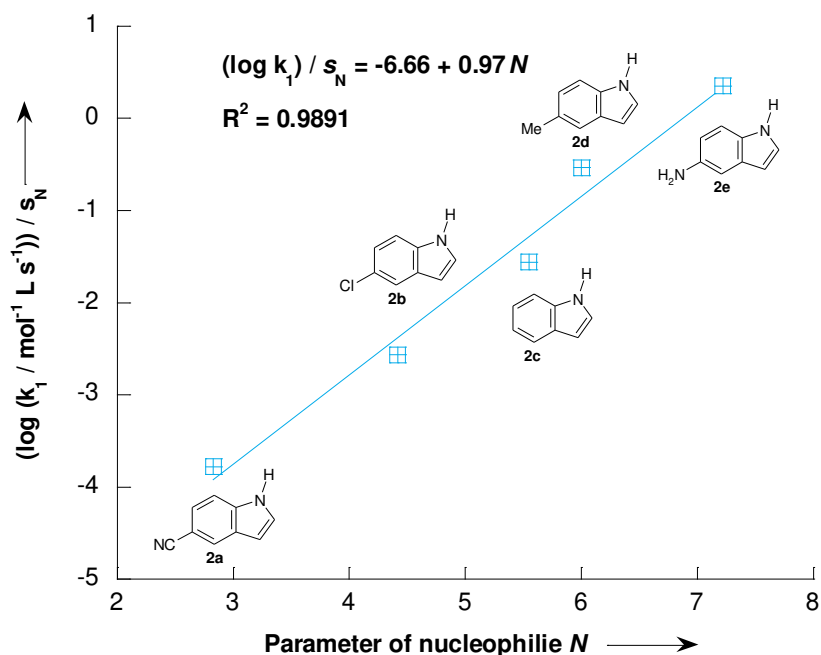

Figure 8. Plot of the rate constants (log k_1)/s_N for the reaction of the of 2-(2',4',6'-trinitrophenyl)-4,6-dinitrobenzotriazole 1-oxide **1** with the reference nucleophiles **2a-e** versus their nucleophilicity parameters N in CH_3CN or CH_2Cl_2 solution at 20 °C.

Figure 9 compares the reactivity of the of 2-(2',4',6'-trinitrophenyl)-4,6-dinitrobenzotriazole 1-oxide **1** with other superelectrophiles, namely tetrazolopyridine **8**, 4,6-dinitrobenzofuroxan **9**, 6-cyano-4-nitrobenzofuroxan **10**, 4,6-dinitrobenzofurazan **11**, and 2,4,6-trinitrobenzene **12** (Terrier et al. 2005), along with superelectrophiles previously investigated by Mayr and co-workers, such as 2-phenyl-1,3-dithianylium ion **13**, (Mayr et al. 2003) and benzhydrylium ion **14** (Ammer et al. 2012). Figure 9 reveals that the benzotriazole **1** ($E = -6.87$) exhibits electrohilicity comparable to 6-cyano-4-nitrobenzofuroxan **10** ($E = -7.01$) and 2-phenyl-1,3-dithianylium ion **13** ($E = -6.43$), but is roughly 1.5 to 2 orders of magnitude less reactive than tetrazolopyridine **8** ($E = -4.67$), 4,6-dinitrobenzofuroxan **9** ($E = -5.06$), and 4,6-dinitrobenzofurazan **11** ($E = -5.46$). On the other hand, our electrophile **1** is 6.3 orders of magnitude more reactive than 2,4,6-trinitrobenzene **12** ($E = -13.19$), the conventional aromatic electrophile in nucleophilic addition or substitution processes (Buncel et al. 2010; Ayachi et al. 2020). As seen in Figure 9, the difference in reactivity between benzotriazole **1**

13

and benzhydrylium ion ($E = 8.02$), the weakest known superelectrophiles to date, is approximately 15 units of E.
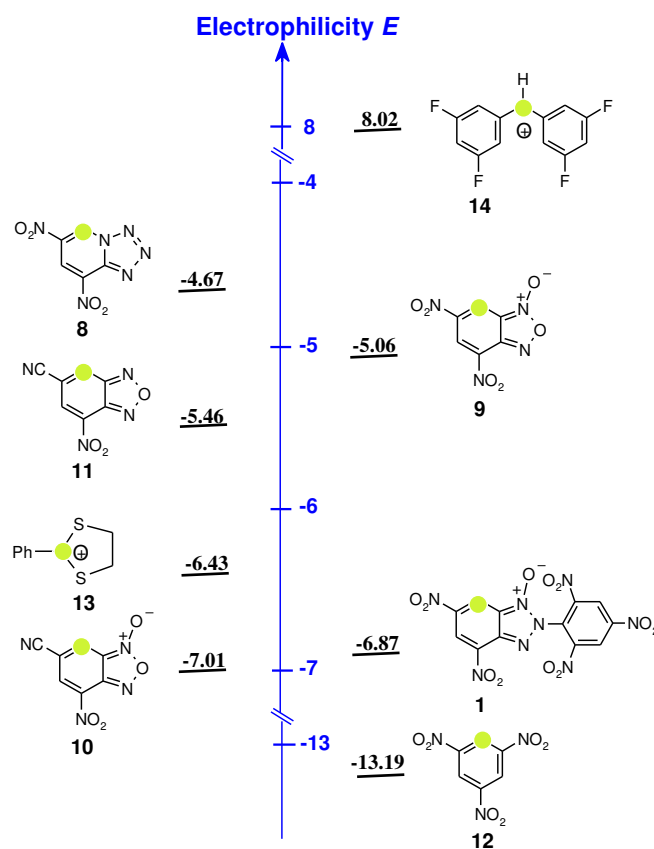
Figure 9. Comparison of the electrophilicity of 2-(2',4',6'-trinitrophenyl)-4,6-dinitrobenzotriazole 1-oxide **1** with those of other superelectrophiles reported by our laboratory and Mary's team.

2.5. Correlation between Nucleophilicity parameter (N) and global electrophilicity index (ω^{-1})

The primary focus of the present study was to establish and to explore a relationships between theoretical results and experimental data to predict the unknown nucleophilicity parameters (N) values of some 5-R-substituted indoles in acetonitrile solution. In this context, a theoretical study was conducted using density functional theory (DFT) to calculate the global nucleophilicity index (ω^{-1}) for the series of indoles **2a-e** considered in the present study. This calculation followed the model developed by Parr and co-workers (Eq. (6)) (Parr et al. 1999).

$$\omega^{-1} = 2\eta/\mu^2 \tag{6}$$

The electronic chemical potential (μ) and chemical hardness (η) may be approached in terms of the one-electron energies ε_{HOMO} and ε_{LUMO} of the HOMO and LUMO frontier molecular

14

orbitals, respectively, according to the approximate expressions (7) and (8) (Parr and Pearson 1983; Parr and Yang 1989). The values of global nucleophilicity index (ϖ^{-1}) obtained in this manner are listed in Table 3 for the various indoles **2a-e** .

$$\mu \approx (\varepsilon_{HOMO} + \varepsilon_{LUMO})/2 \tag{7}$$

$$\eta \approx (\varepsilon_{LUMO} - \varepsilon_{HOMO}) \tag{8}$$

Table 3. Values of ε_{HOMO}, ε_{LUMO}, μ, η, and ω^{-1} for the substituted indoles **2a-e** calculated in this work at the B3LYP/6-311g(d,p) level of theory in acetonitrile.

5-R-indole		ε_{HOMO} (eV)	ε_{LUMO} (eV)	μ (eV)	η (eV)	ω^{-1} (eV^{-1})
2a	CN	−6.216	−1.261	−3.7385	4.9550	0.709
2b	Cl	−6.037	−0.855	−3.4460	5.1820	0.873
2c	H	−5.827	−0.579	−3.2030	5.2480	1.023
2d	CH$_3$	−5.778	−0.519	−3.1485	5.2590	1.061
2e	NH$_2$	−5.289	−0.502	−2.8955	4.7870	1.142

Analysis of the data summarized in Tables 2 and 3 revealed the exitence of a direct relationship between the nucleophilicity parameter N and the global nucleophilicity index ω^{-1}, as shown in Figure 10. The linear dependence is described by Equation (9). Similar relationships between parameters N and ω^{-1} have also been reported by many authors (Raissi et al. 2023). The data in Table 4 serve as an illustration in this regard.

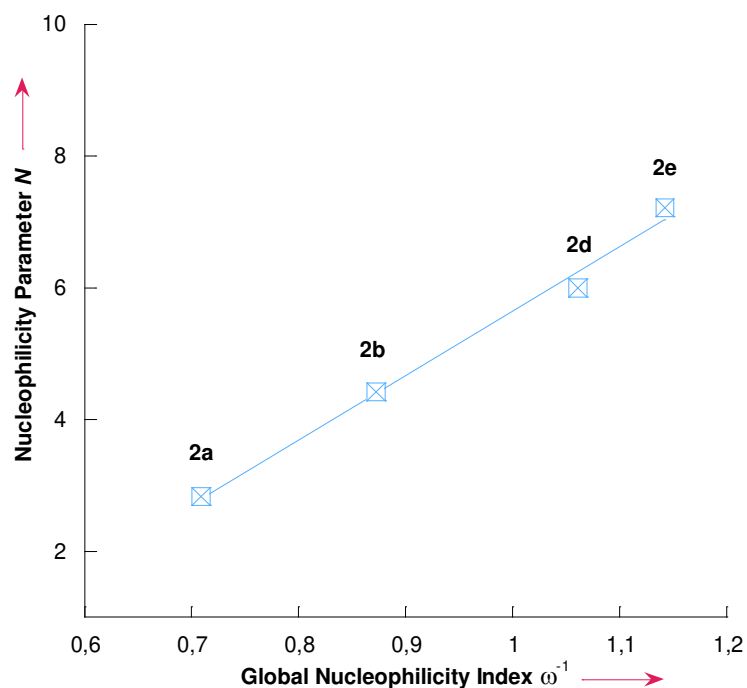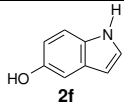$$N = -4.14 + 9.79\ \omega^{-1} \qquad (R^2 = 0.9957) \tag{9}$$
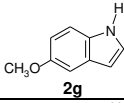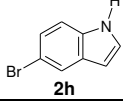
Figure 10. Correlations between global nucleophilicity index (ω^{-1}) calculated at B3LYP/6-311g(d,p) level for the 5-R-substituted indoles **2a-e** listed in Table 3 and their experimentally determined nuleophilicities N.

Table 4. Relationships N $vs.$ ω^{-1} and correlation oefficients of some representative nuclepphiles in various solvents.

Nucleophile	Solvent	Relationship (Correlation Coefficient)	Ref
	Methanol	$N = 3.87\omega^{-1} + 10.92$ (0.9964)	Raissi et al. 2023
	Acetonitrile	$N_{Theo} = 0.127\,N_{Exp} + 1.96$ (0.98)	Yao et al. 2022
	Acetonitrile	$N_{Theo} = 0.068 N_{Exp} + 3.47$ (0.99)	
	Methanol	$N = -2.427\omega^{-1} + 16.649$ (0.9990)	Necibi et al. 2023
	Water	$N_{Mayr} = 9.09\omega^{-1} + 32.27$ (0.99) Using HF /6-31G (d) level of theory	Chamorro et al. 2009
		$N_{Mayr} = 2.94\omega^{-1} + 36.18$ (0.99) Using B3LYP/6-31G (d) level of theory	
	Methanolic Acetonitrile Solutions	$N = 1.164\omega^{-1} - 16.736$ (0.9988)	Souissi et al. 2020

To evaluate the performance of the Equation (9), we recalculated the nucleophilicity parameter N of the three 5-R-substitutd indoles **2f-h** (**2f**: X = OH, **2g**: X = OCH₃, and **2h**: X = Br) whose experimental data are available (Lakhdar et al. 2006). We found that the predicted N values are consistent with the expected values reported in the literature as depicted in Table 5. Note that, the global nucleophilicity ω^{-1} values have been calculated in acetonitrile by quantum chemical calculations at the B3LYP/6-311g(d,p) level of theory using Gaussian 09 (See Table S2, Suporting Informtion,). This result indicates that equation (9) can successfully predict the values of other 5-R-substituted indoles from their known ω^{-1} values in acetonitrile solutions.

Table 5. Experimental and theoretical nucleophilicity parameter N and global nucleophilicity ω^{-1} values for the 5-R-substituted indoles **2f-h**.

5-R-substituted indole	ω^{-1} (eV^{-1}) [a]	N
2f	1.069	6.31[b] (6.44)[c]
2g	1.040	6.02[b] (6.22)[c]
2h	0.873	4.39[b] (4.38)[c]

[a]Values determined in this work at the B3LYP/6-311g(d,p) level of theory in CH₃CN.
[b]Values calculated in this work from Eq. (9) in CH₃CN.
[c]N values in CH₃CN were taken from ref (Lakhdar et al. 2006).
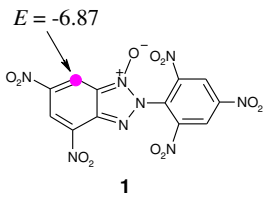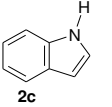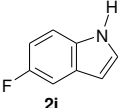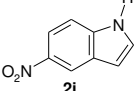
2.6. Application: Nucleophile specific parameters N and s$_N$ of other unknown indoles

Most importantly, correlation (9) can be serve as a reliable model for predicting the unknown nucleophilicity N values of several 5-R-substituted indoles. Based on this correlation, the N values of indole **2c**, 5-fluoro-indole **2i**, and 5-nitro-indole **2j** have been evaluated using their ω^{-1} values calculated in the present work at the B3LYP/6-311g(d,p) level of theory (See Table 6, and Table S2, Suporting Informtion).

In order to quantify the nucleophile-specific slope parameters s_N of indoles **2c**, **2i** and **2j** we have studied the kinetics of their electrophilic heteroaromatic substitution reactions with the benzotriazole **1** in acetonitrile solution at 20 °C (See Table 6, and Figures S1 and S2,

Supporting Information). The resulting second-order rate constants k_1, were employed to evaluate the parameters s_N of these indoles **2c**, **2i** and **2j** according to the correlation equation log k (20 °C) = s_N (N + E), their N values previously predicted and the parameter E of **1**. The detailed results are listed in Table 6. Also to be noted is that the parameters s_N determined in the present work are of similar magnitude than those of the 5-R-substituted indoles ($s_N \approx 1.10$ in acetonitrile) considered in this present work (Lakhdar et al. 2006).

Table 6. Second-order rate constants k_1 for the reactions of benzotriazole **1** with 5-R-substituted indoles **2c**, **2i**, and **2j** and their ω^{-1}, N, and s_N parameters in acetonitrile solution at 20 °C.

Electrophile	Indole	ω^{-1} (eV^{-1})[a]	k_1 (M^{-1} s^{-1})[b]	N[c]	s_N[d]
E = -6.87 **1**	**2c**	1.023	8.91 x 10^{-2}	5.87	1.05
	2i	0.913	4.80 x 10^{-3}	4.80	1.12
	2j	0.391	1.76 x 10^{-8}	−0.31	1.08

[a]Values determined in this work at the B3LYP/6-311g(d,p) level of theory in CH$_3$CN.
[b]Values measured in this work from the slope of plots of k_{obsd} *vs.* [5-R-indole] in CH$_3$CN.
[c]Values calculated in this work from Eq. (9) in CH$_3$CN.
[d]s_N values calculated from Equation (1) using the E parameter of **1**, the second-order rate constants k_1 measured in this work, and the reactivity parameters N of **2c**, **2i** and **2j** listed in this Table 6.

3. Conclusion

The electrophilic reactivity of 2-(2',4',6'-trinitrophenyl)-4,6-dinitrobenzotriazole 1-oxide **1** was determined by analyzing the kinetics of their reactions with a series of 5-R-substituted indoles **2a-e** in acetonitrile or dichloromethane at 20 °C following Mayr's approach. Detailed calculations were carried out to better understand the observed SET mechanism. Using density functional theory (DFT) and Parr's approach, we deteremined the global nucleophilicity index ω^{-1} of ten 5-R-substituted indoles. On the other hand, N values of three indoles (R = OH, OCH$_3$, and Br) were predicted based on the N *vs.* ω^{-1} correlation obtained in the present work, and the results aligned with those reported in the literature. Additionally, we also predicted the unknown nucleophile specific parameters N and s_N of three new 5-R-

substituted indoles (R = NO$_2$, F and H) in acetonitrile for the first time using Mayr's equation and our N *vs.* ω^{-1} correlation.

4. Experimental Section

4.1. Materials

All spectrophotometric measurements were conducted using a UV-1650 Shimadzu spectrophotometer equipped with a Peltier temperature controller (model TCC-240 A), capable of maintaining the temperature within 0.1 K.

The 2-(2',4',6'-trinitrophenyl)-4,6-dinitrobenzotriazole 1-oxide **1**, was prepared as previously described (Vichard et al. 2001). All the 5-R-substituted indoles **2a-k** are commercial products available of the highest quality (99.9%, extra dry) and were used as received. Acetonitrile (Aldrich, HPLC: 99.9%) of the highest quality was used without further purification. Dichloromethane was freshly distilled over CaH$_2$ prior to use. (99.9%, extra dry)

4.2. Kinetic Measurements

All the reactions in the present study obeyed pseudo first-order kinetics in the presence of excess indole. The pseudo first-order rate constants (k$_{obsd}$) were calculated using (Eq.10), where A$_\infty$ refers to the absorbance of the product **3** at the completion of the reaction, A$_o$ refers to the absorbance at zero time, and A$_t$ refers to the absorbance at time t. Plotting Ln(A$_\infty$-A$_t$) versus t yielded highly linear curves with correlation coefficients usually exceeding 0,98…. The measured first-order rate constants, k$_{obsd}$, values and detailed reaction conditions are summarized in Table S1 in the Supporting Information.

$$\text{Ln } (A_\infty - A_t) = -k_{obsd} \, t + \text{Ln } (A_\infty - A_o) \tag{10}$$

4.3. Methods and Computational Aspects

The molecular structures were optimized using the Gaussian 09 program (Frisch et al. 2009). Complete calculations in polar acetonitrile (CH$_3$CN) were performed using the conductor-like polarizable continuum model (CPCM) (Mishra et al. 2016) and density functional theory (DFT) with the B3LYP (Becke three-parameter Lee-Yang-Parr) exchange-correlation functional (Becke 1993; Lee et al. 1988), in conjunction with the 6-311g(d,p) basis set. The

19

generated output files were utilized in the Gauss View (5.0.8) program (Govindarajan et al. 2012). Based on the molecular optimized geometry, electronic properties, including highest occupied molecular orbital (ε_{HOMO}) and lowest unoccupied molecular orbital (ε_{LUMO}) energy levels, were calculated. Time-dependent density functional theory (TD-DFT) was employed as a suitable framework for predicting the experimental UV-vis optical absorption spectrum of studied compound. Density of states (DOS) digrams were generated using Gaussum program (O'Boyle et al. 2007).

Supporting Information Available

Table S1. Concentrations and the measured rate constants, k_{obsd}, for the individual kinetic experiments values for reactions for the reactions of the 2-(2',4',6'-trinitrophenyl)-4,6-dinitrobenzotriazole 1-oxide **1** with a series of 5-R-substituted indoles **2a-e** (R = CN, Cl, H, CH_3 and NH_2) in CH_3CN or CH_2Cl_2 at 20 °C.

Table S2. Values of ε_{HOMO}, ε_{LUMO}, μ, η, and ω^{-1} for the 5-R-substituted indoles **2f-j** calculated in this work at the B3LYP/6-311g(d,p) level of theory in CH_3CN.

Figure S1. Plot of the first-order rate constants k_{obsd} *vs*. the concentration of 5-fluoro-indole **2i** in acetonitrile solution at 20 °C.

Figure S2. Plot of the absorbance at λ_{max} = 468 nm versus time observed for the reaction of 2-(2',4',6'-trinitrophenyl)-4,6-dinitrobenzotriazole 1-oxide **1** (3 x 10^{-5}) in the presence of 5-nitro-indole **2j** (1 mol L^{-1}) in acetonitrile solution at 20 °C.

Conflicts of interest

The authors declare no competing interests.

Author contributions

Ons Amamou, Amel Hedhli, and Takwa Slama achieved their experimental works with the help of Taoufik Boubaker. Theoretical calculations were conducted by Sahbi Ayachi. The manuscript was jointly written and arranged under TB, and SA guidance.

References

1   Ammer J, Nolte C, Mayr H (2012) Free Energy Relationships for Reactions of Substituted Benzhydrylium Ions: From Enthalpy over Entropy to Diffusion Control. J Am Chem Soc 134:13902-13911. https://doi.org/10.1021/ja306522b.

2   Ayachi H, Raissi H, Mahdhaoui F, Boubaker T (2020) Electrophilic reactivities of 7-L-4-nitrobenzofurazans in σ-complexation processes: Kinetic studies and structure–reactivity relationships. Int J Chem Kinet 52:655-668. https://doi.org/ 10.1002/ kin.21390.

3   Ayachi S, Bouzakraoui S, Hamidi M, Bouachrine M, Molinié P, Alimi K (2006) Prediction of electropolymerization mechanisms of two substituted phenylene: Poly-3-methoxy-toluenes (P3mt$_1$ and P3mt$_2$). J Appl Polym Sci 100:57-64. https://doi.org/ 10.1002/app.22640.

4   Becke AD (1993) Density-functional thermochemistry III. The role of exact exchange. J Chem Phys 98: 5648-5652. https://doi.org/10.1063/1.462066.

5   Ben Salah S, Boubaker T, Goumont R (2017) Kinetic and Mechanism of Phenoxide Anions Addition to 4-nitrobenzofurazan in Aqueous Solution. Can J Chem 95:723-728. https://doi.org/10.1139/cjc-2016-0182.

6   Boubaker T, Chatrousse AP, Terrier F, Tangour B, Dust JM, Buncel E (2002) Water and Hydroxide ion Pathways in the σ-Complexation of Superelectrophile 2-Aryl-4,6-Dinitrobenzotriazole 1-Oxides in Aqueous Solution. A kinetic and Thermodynamic Study. J Chem Soc Perkin Trans 2:1627-1633. https://doi.org/10.1039/B201731H.

7   Boubaker T, Goumont R, Jan E, Terrier F (2003) An extremely highly electrophilic heteroaromatic structure: 4,6-dinitrotetrazolo[1,5-a] pyridine. Org Biomol Chem 1: 2764-2770. https://doi.org/10.1039/B306437A.

8   Buncel E, Terrier F (2010) Assessing the Superelectrophilic Dimension Through σ-Complexation, S$_N$Ar and Diels–Alder Reactivity. Org Biomol Chem 8:2285-2308. https://doi.org/10.1039/B923983A.

9   Chamorro E, Duque-Noreña M, Pérez P (2009) Further relationships between theoretical and experimental models of electrophilicity and nucleophilicity. J Mol Struct 901145:152. https://doi.org/10.1016/j.theochem.2009.01.014.

10 Corral-Bautista F, Appel R, Frickel JS, Mayr H (2015) Quantification of Ion-Pairing Effects on the Nucleophilic Reactivities of Benzoyl- and Phenyl-Substituted Carbanions in Dimethylsulfoxide. Chem Eur J 21:875-884. https://doi.org/10.1002/chem.201404500.

11 Echaieb A, Gabsi W, Boubaker T (2014) Nucleophilic Substitution Reactions of 2-Methoxy- 3-X-5-nitrothiophenes: Effect of Substituents and Structure–Reactivity Correlations. Int J Chem Kinet 46:470-476. https://doi.org/10.1002/kin.20863.

12 El Guesmi N, Boubaker T, Goumont R, Terrier F (2009) The ambident reactivity of 2,4,6-tris(trifluoromethanesulfonyl) anisole in methanol: Using the SO_2CF_3 froup as a tool to reach the superelectrophilic dimension in σ-complexation processes. Chem Eur J 15: 12018-12029. https://doi.org/10.1002/chem.200901123.

13 El Guesmi N, Boubaker T, Goumont R (2010) Activation of the aromatic system by the SO_2CF_3 group: Kinetics study and structure-reactivity relationships. Int J Chem Kinet 42:203-210. https://doi.org/10.1002/kin.20446.

14 El Guesmi N, Boubaker T, Goumont R (2013) Single electron transfer in S_NAr process: Reactions of 2,4,6-tris(trifluoromethanesulfonyl)anisole with anilines in dimethyl sulfoxide. Prog React Kinet Mech 38:130-142. https://doi.org/10.3184/146867813X13642226149123.

15 Frisch MJ, et al. (2009) Gaussian 09, Revision A.01. Gaussian, Inc., Wallingford. http://www. gaussian. com/.

16 Gabsi W, Boubaker T, Goumont R (2016) Azo-coupling Reactions of para-X-benzenediazonium cations with 3-ethoxythiophene in Acetonitrile. Int J Chem Kinet 48:266-273. https://doi.org/10.1002/kin.20989.

17 Gabsi W, Essalah K, Goumont R, Tangour B, Boubaker T (2018) The ambient electrophilic behavior of 5-nitro-3-X-thiophenes in σ-complexation processes. Int J Chem Kinet 50:659-669. https://doi.org/10.1002/kin.21190.

18 Govindarajan M, Periandy S, Carthigayen K (2012) FT-IR and FT-Raman spectra, thermo dynamical behavior, HOMO and LUMO, UV, NLO properties, computed frequency estimation analysis and electronic structure calculations on α-bromotoluene. Spectrochim Acta A Mol Biomol Spectrosc 97:411-422. https://doi.org/10.1016/j.saa.2012.06.028.

19 Hensinger MJ, Eitzinger A, Trapp O, Ofial AR (2023) Nucleophilicity of 4-(Alkylthio)-3-imidazoline Derived Enamines. Chem Eur J 29:3-9. https://doi.org/10.1002/chem.202302764.

20 Hunter A, Renfrew M, Rettura D, Taylor JA, Whitmore JM, Williams A (1995) Stepwise versus Concerted Mechanisms at Trigonal Carbon: Transfer of the 1,3,5-Triazinyl Group between Aryl Oxide Ions in Aqueous Solution. J Am Chem Soc 117: 5484-5491. https://doi.org/10.1021/ja00125a008.

21 Jamaoui I, Boubaker T, Goumont R (2013) Nonlinear Brønsted and Hammett Correlations Associated to Reactions of 4-chloro-7-nitrobenzofurazan with Anilines in dimethyl sulfoxide solution. Int Chem Kinet 45:152-160. https://doi.org/10.1002/kin.20751.

22 Jennings P, Jones AC, Mount AR, Thomson AD (1997) Electrooxidation of 5-substituted indoles. J Chem Soc Faraday Trans 93:3791-3797. https://doi.org/10.1039/A703128I.

23 Justel PM, Pignot CD, Ofial AR (2021) Nucleophilic Reactivities of Thiophenolates. J Org Chem 86:5965-5972.https://doi.org/10.1021/acs.joc.1c00025.

24 Lakhdar S, Westermaier M, Terrier F, Goumont R, Boubaker T, Ofial AR, Mayr H (2006) Nucleophilic reactivities of indoles. J Org. Chem 71:9088-9095. https://doi.org/10.1021/jo0614339.

25 Lee C, Yang W, Parr RG (1988) Development of the Colle-Salvetti correlation-energy formula into a functional of the electron density. Phys Rev B 37:785-789. https://doi.org/10.1103/PhysRevB.37.785.

26 Li L, Mayer RJ, Stephenson DS, Mayer P, Ofial AR, Mayr H (2022) Quantification of the Electrophilicities of Diazoalkanes: Kinetics and Mechanism of Azo Couplings with Enamines and Sulfonium Ylides. Chem Eur J 28:1-13. https://doi.org/10.1002/chem.202201376.

27 Mahdhaoui F, Dhahri N, Boubaker T (2016) Single Electron Transfer in σ-complexation Reactions of 2,6-dimethoxy-3,5-dinitropyridine with Para-X-phenoxide Anions in Aqueous Solution. Int J Chem Kinet 48:523-530. https://doi.org/10.1002/kin.21011.

28 Mayr H, Kempf B, Ofial AR (2003) π-Nucleophilicity in Carbon-Carbon Bond-Forming Reaction. Acc Chem Res 36:66-77. https://doi.org/10.1021/ar020094c.

29 Mayr H, Patz M (1994) Scales of Nucleophilicity and Electrophilicity: A System for Ordering Polar Organic and Organometallic Reactions. Angew Chem Int Ed Engl 33:938-957. https://doi.org/10.1002/anie.199409381.

30 Miar M, Shiroudi A, Pourshamsian K, Oliaey AR, Hatamjafari F (2021) Theoretical investigations on the HOMO–LUMO gap and global reactivity descriptor studies, natural bond orbital, and nucleus-independent chemical shifts analyses of 3-phenylbenzo[d]thiazole-2(3H)-imine and its para-substituted derivatives: Solvent and substituent effects. J Chem Res 45:147-158. https://doi.org/10.1177/17475198209320.

31 Mishra V, Raghuvanshi A, Saini AK, Mobin SM (2016) Anthracene derived dinuclear gold (I) diacetylide complexes: Synthesis, photophysical properties and supramolecular interactions. J Org Chem 813:103-109. https://doi.org/10.1016/j.jorganchem.2016.04.013Get rights and content.

32 Necibi F, Salah SB, Hierso JC, Fleurat-Lessard P, Ayachi S, Boubaker T (2023) Nucleophilicity Parameters for Nitroalkyl Anions in Methanol and Structure-Reactivity Analysis. Chemistry Select 8:1-8. https://doi.org/10.1002/slct.202203590.

33 Necibi F, Salah SB, Roger J, Hierso JC, Boubaker T (2020) Ambident electrophilicity of 4-nitrobenzochalcogenadiazoles: Kinetic studies and structure-reactivity relationships. Int J Chem Kinet 52:669-680. https://doi.org/10.1002/kin.21391.

34 O'Boyle NM (2007) GaussSum, Version 2.0.5 Available at http://gausssum.sf.net.

35 Parr RG, Pearson RG (1983) Absolute Hardness: companion parameter to absolute electronegativity. J Am Chem Soc 105:7512-7516. https://pubs.acs.org/doi/pdf/10.1021/ja00364a005.

36 Parr RG, Szentpály L.V, Liu S (1999) Electrophilicity Index. J Am Chem Soc 121:1922-1924. https://doi.org/10.1021/ja983494x.

37 Parr RG, Yang W (1989) Density Functional Theory of Atoms and Molecules; Oxford University Press: New York. doi:10.1007/978-94-009-9027-2_2.

38 Raissi H, Ayachi H, Mahdhaoui F, Ayachi S, Boubaker T (2021) Relationships between experimental and theoretical scales of electrophilicity of 7-L-4-nitrobenzofurazans. J Mol Struct 1224:128843-128853. https://doi.org/10.1016/j.molstruc.2020.128843.

39 Raissi H, Chérif I, Aribi I, Ayachi H, Haj Said A, Ayachi S, Boubaker T (2022) Structure-property relationships in para-substituted nitrobenzofurazans: electrochemical, optical, and theoretical analysis. Chemical Papers 76:4059–4080. https://doi.org/10.1007/s11696-022-02150-y.

40 Raissi H, Jamaoui I, Goumont R, Boubaker T (2017) Kinetic Studies on S_NAr Reactions of Substituted Benzofurazan Derivatives: Quantification of the Electrophilic Reactivities and Effect of Amine Nature on Reaction Mechanism. Int J Chem Kinet 49: 835-846. https://doi.org/10.1002/kin.21131.

41 Raissi H, Mahdhaoui F, Ayachi S, Boubaker T (2023) Solvent efect, quantifcation and correlation analysis of the nucleophilicities of cyclic secondary amines. Chemical Papers 77:307-319. https://doi.org/10.1007/s11696-022-02483-8.

42 Rammah M, Mahdhaoui F, Ayachi S, Boubaker T (2022) Exploring the reactivity of benzotriazole derivatives: Mayr's approach and density functional theory analysis. J Mol Struct 1247:131310. https://doi.org/10.1016/j.molstruc.2021.131310.

43 Rammah M, Mahdhaoui F, Gabsi W, Boubaker T (2021) Quantification of the Electrophilic Reactivities of Benzotriazoles and Structure-Reactivity Relationships. Chem Select 6:4424-4431. https://doi.org/10.1002/slct.202100568.

44 Safi Z, Wazzan N (2023) Substitution effect on the adiabatic ionization potential, vertical ionization potential, electrophilicity, and nucleophilicity of some hydantoin drug derivatives: Computational study. J Phy Org Chem 36:4565-4581. https://doi.org/10.1002/poc.4565.

45 Salah SB, Necibi F, Goumont R, Boubaker T (2020) Electrophilicities of 4-Nitrobenzochal cogenadiazoles. Chem Select 5:7648-7657. https://doi.org/10.1002/slct.202001928.

46 Slama T, Amamou O, Hedhli A, Guillemin JC, Ayachi S, Boubaker T (accepted 2023) Electrophilicity, Mechanism and Structure-Reactivity Relationships of Cyclic Secondary Amines Addition to 2-Methoxy-3,5-dinitropyridine. J Mol Struct. https://doi.org/10.1016/j.molstruc.2023.137258.

47 Souissi S, Gabsi W, Echaieb A, Hierso JC, Fleurat-Lessard P, Boubaker T (2020) Influence of solvent mixture on nucleophilicity parameters: The case of pyrrolidine in methanol-acetonitrile. RSC Advances 10:28635-28643. DOI: 10.1039/D0RA06324J.

48 Terrier F (2013) Modern Nucleophilic Aromatic Substitution; John Wiley & Sons: Weinheim.

49 Terrier F, Mokhtari M, Goumont R, Halle JC, Buncel E (2003) Hight Bronsted β_{nuc} values in S_NAr displacement. An indicator of the set pathway. Org Biomol Chem 1:1757-1763. https://doi: 10.1039/b301031g.

50 Terrier F, Pouet MJ, Halle JC, Hunt S, Jones JR, Buncel E (1993) Electrophilic Heteroaromatic Substitutions : Reactions of 5-X-Substituted indoles with 4,6-Dinitrobenzofuroxan. J Chem Soc Perkin Trans 2:1665-1672. https://doi.org/10.1039/P29930001665.

51 Terrier T, Lakhdar S, Boubaker T, Goumont R (2005) Ranking the Reactivity of Superelectrophilic Heteroaromatics on the Electrophilicity Scale. J Org Chem 70:6242-6253. https://doi.org/10.1021/jo0505526.

52 Timofeeva DS, Ofial AR, Mayr H (2018) Kinetics of Electrophilic Fluorinations of Enamines and Carbanions: Comparison of the Fluorinating Power of N–F Reagents. J Am Chem Soc 140:114746-11486. https://doi.org/10.1021/jacs.8b07147.

53 Vichard D, Boubaker T, Terrier F, Pouet MJ, Dust JM, Buncel E (2001) The versatile reactivity of 2-aryl-4,6-dinitrobenzotriazole 1-oxides in Diels-Alder type condensations between superelectrophillicity and pericyclic reactivity. Can J Chem 79:1617-1623. https://doi.org/10.1139/v01-020.

54 Yao L, Long Z, Sanzhong L (2022) Bond Energies of Enamines. *ACS Omega* 7:6354-6374. https://doi.org/10.1021/acsomega.1c06945.

55 Zhuo LG, Liao W, Yu ZX A (2012) Frontier Molecular Orbital Theory Approach to Understanding the Mayr Equation and to Quantifying Nucleophilicity and Electrophilicity by Using HOMO and LUMO Energies. Asian J Org Chem 1:336-345. https://doi.org/10.1002/ajoc.201200103.

Supplementary Files

This is a list of supplementary files associated with this preprint. Click to download.

- SupportingInformation.doc